

A MEASUREMENT OF THE PHASE AND THE MODULUS OF η_{00}

J. Chollet^{*}, J.-M. Gaillard, M.R. Jane[/], T.J. Ratcliffe,
J.-P. Repellin^{*}, K.R. Schubert, B. Wolff^{*}

CERN, Geneva, Switzerland.

1. INTRODUCTION

The aim of the experiment was to determine the phase of η_{00} in order to resolve the ambiguity between the two solutions of the Wu and Yang⁽¹⁾ triangle. Whatever the value of $|\eta_{00}|$, two solutions arise in the determination of the triangle using $|\eta_{+-}|$, φ_{+-} and $|\eta_{00}|$. Using the known values of $|\eta_{+-}|$ and φ_{+-} , the solutions present the interesting feature that the phase difference $(\varphi_{00})_{\text{Sol.1}} - (\varphi_{00})_{\text{Sol.2}}$ is close to 180° .

In view of the present uncertainty on $|\eta_{00}|$, the data was analysed to extract also that quantity. The value of $|\eta_{00}|$ was left as a free parameter for the analysis, and both $|\eta_{00}|$ and φ_{00} have been determined. The apparatus has now been modified in order to obtain a more precise value for $|\eta_{00}|$ and data taking is underway.

2. EXPERIMENTAL SETUP

A neutral beam taken at 17° from an external target at the CERN PS was passed through 5 cm of lead and a sweeping magnet to remove gamma rays and charged particles. The full beam di-

* Visitor from Laboratoire de l'Accélérateur Lineaire, Orsay 91, France.

/ Visitor from Rutherford High Energy Laboratory, Chilton, Berkshire, England.

mensions, defined by two tapered collimators each three metres long, were 9 cm wide and 8 cm high at the entrance of the detection equipment situated 18 metres from the target.

The experiment was run with a beam intensity of about 10^{11} protons hitting the target, giving approximately $5 \cdot 10^3 K_L^0$ per burst down the beam line, at an average momentum of 2 GeV/c.

Figure 1 is a diagram of the equipment. The spark chamber 3 plate modules have been described elsewhere⁽²⁾; they were placed in banks of 26 modules (52 gaps) on either side of the beam. The distance from the inner edge of the chambers to the central beam line was 6 cm. The first eighteen modules on each side were made with 5-mm thick aluminium plates and the last eight modules with 5-mm brass plates, making a total spark-chamber thickness of 11.0 radiation lengths. The first 3 radiation lengths (aluminium chambers) occupied 105 cm, giving an average radiation length of 35 cm; the last 8 radiation lengths (brass chambers) occupied 32 cm, giving an average radiation length of 4 cm.

Three layers of scintillation counters were inserted on both sides after the eighth, thirteenth and eighteenth aluminium modules. The trigger was given by a six-fold coincidence composed as follows:

- a) a four-fold coincidence between left-upper, left-lower, right-upper and right-lower quadrants.

The signal from each quadrant was from either one, or both, of the first and third counter layers.

b) in addition, a signal from the second layer was required from both sides.

This arrangement was designed to favour four gamma ray events in which one gamma ray converted in the aluminium section of each quadrant of the spark chamber.

Scintillation counters A_3 were put in front of the spark chambers and used to veto counts from charged particles. A counter A_1 vetoed charged particles or converted gamma rays coming out of the regenerator. The anticoincidence counters A_2 , A'_2 , A_4 comprised layers of lead or steel converters and scintillation counters in order to detect and veto additional gamma rays produced by the decay $K_L^0 \rightarrow 3\pi^0$ which was the main source of background.

A lead wall 20 cm thick with a tapered hole in its centre defined the beginning of the decay region. The minimum dimensions of the hole were 15 cm wide and 13.5 cm high, so that the edges of the hole were sufficiently far from the beam. A copper regenerator 12 cm thick had six fixed positions upstream from the wall and the anticounter A_1 was moved with it. The six positions were uniformly spread over 60 cm.

Behind the chambers a neutron monitor measured the beam intensity used in each position. This monitor was checked several times during the runs against a monitor looking directly at the target. The ratio of these two monitors was found to be the same within ± 2 per cent for all six positions.

The aluminium chambers were photographed with 90° stereo and the brass chambers in side view. Adox track-chamber

70-mm film was used. About 240,000 pictures were taken; the amount of time spent in each position was a function of its distance from the lead wall (5% for the nearest position up to 40% for the upstream position).

The veto effect of every group of anticounters was continuously recorded. In parallel, the dead time effect of the same groups of counters were also continuously measured in order to correct for it. The total dead time effect was typically 20%.

3. FILM SCANNING AND MEASUREMENT

The scanning criteria used were very similar to those of a previous experiment⁽³⁾. The events selected were measured on hand operated image plane digitizers, and the following quantities were determined for each shower: conversion point, initial direction, and shower energy. The accuracy to which the conversion point could be determined was about ± 2 mm in real space.

In order to determine the shower energies from spark counting, a linear form was adopted as in reference (3):

$$E_{\gamma} = A N_A + B N_B$$

where N_A and N_B are the numbers of sparks occurring in aluminium and brass respectively; A and B are two constants which have been determined experimentally by comparing the energy E_{ϕ} of the π^0 with $E_{\gamma\gamma}$ deduced from spark counting in selected $K_S^0 \rightarrow 2 \pi^0$ regenerated events:

$$E_{\phi} = m_{\pi^0} \frac{(E_1/E_2)^{1/2} + (E_2/E_1)^{1/2}}{2 \sin(\phi/2)}$$

where ϕ is the opening angle of the π^0 , E_1 and E_2 are the gamma ray energies determined from spark counting. The fitting procedure has shown that $(E_\phi - E_{\gamma\gamma})/E_{\gamma\gamma}$ has a standard deviation of 17%.

4. DATA ANALYSIS AND RESULTS

Two types of analysis are presented below, based on about 80% of the data. They were made on the assumption that the four gamma rays observed originate from the decay of two neutral pions. There are three possible ways to combine these four gamma rays in pairs to form a " $2\pi^0$ event"; the analysis of the events and the Monte Carlo simulation have shown that 96% of the $2\pi^0$ events detected by the apparatus belong to one particular combination; the preferred pairing is such that the gamma rays from one π^0 convert in the chambers on the left and those from the other π^0 in the chambers on the right. The results presented below were obtained using the preferred pairing. After a first selection all the events entering into the plots were checked by physicists on the scanning table.

4.1 $2\pi^0$ DECAY INTENSITY AFTER A REGENERATOR

The problem of the two pion decay intensity after a regenerator, including incoherent regeneration and interference effects, have been studied by different authors (4, 5). In the case of this experiment, the $2\pi^0$ decay intensity per unit K_S^0 lifetime can be expressed as:

$$\begin{aligned}
 I_{\pi^0\pi^0} \propto & |s|^2 e^{-(z-z_R)/\Lambda_S} \left\{ \sum_{n=0}^{\infty} \epsilon_n \frac{\alpha^n}{n!} \left[1 + \frac{4n\gamma}{\beta^2} - \frac{4n}{\beta} + \frac{4n(n-1)}{\beta^2} \right] \right\} \\
 & + |\eta_{00}|^2 \sum_{n=0}^{\infty} \epsilon_n \frac{\alpha^n}{n!} \\
 & + 2|s||\eta_{00}| e^{-(z-z_R)/2\Lambda_S} \left\{ \cos\left(\delta \frac{z-z_R}{\Lambda_S} + \psi_S - \psi_{00}\right) \sum_{n=0}^{\infty} \epsilon_n \frac{\alpha^n}{n!} \right. \\
 & \left. - 2 \frac{\sigma_D}{\sigma_T} \cos\left(\delta \frac{z-z_R}{\Lambda_S} + \psi_S - \psi_{00} - \psi_{22}\right) \sum_{n=0}^{\infty} \epsilon_{n+1} \frac{\alpha^n}{n!} \right\}
 \end{aligned}$$

where:

$$s = \frac{2\pi i}{k} \Lambda_S N f_{21}(0) \frac{1 - e^{-(1/2 - i\delta)l}}{1/2 - i\delta}$$

where k is the wave number and $f_{21}(0) = [\rho(0) - \bar{\rho}(0)]/2$.

$\Lambda_S = 5.20 p$ (cm) where p is the momentum of the K^0 in GeV/c.

$z =$ coordinate of the decay point along the beam axis.

$z_R =$ coordinate of the exit face of the regenerator.

$\epsilon_0 = \mathcal{E}(z_R, z, p, z', p', 0)$ is the efficiency to detect the decay of a K^0 going along the beam direction with true momentum p , measured momentum p' and measured position z' *

$$\text{For } n \geq 1 \quad \epsilon_n = \int d\psi \int \sin\theta \frac{e^{-\theta^2/2nb^2}}{2\pi nb^2} \mathcal{E}(z_R, z, p, z', p', \theta) d\theta$$

where \mathcal{E} has the same meaning as above but for a K^0 making an angle θ with the beam direction.

$\alpha = NL\sigma_D$ where N is the number of nuclei per unit volume, L the length of the regenerator and σ_D the diffractive cross section.

* All primed quantities refer to measured values; unprimed quantities are the true values.

$\beta = NL\sigma_T$ where σ_T is the total cross section

$$\gamma = \frac{\ell (\delta^2 + 1/4) (1 - e^{-\ell})}{1 + e^{-\ell} - 2 e^{-\ell/2} \cos \delta \ell}, \quad \text{where } \ell = L/\lambda_S$$

and $\delta = (m_{K_L^0} - m_{K_S^0}) \tau_S = 0.465 \pm 0.015$

ψ_S is the phase of S ; $\psi_S = \psi_f + \psi_\delta$ where ψ_f is the phase of $i f_{21}(0)$

ψ_{00} is the phase of η_{00}

ψ_{22} is the phase of $-i f_{22} = -i [f(0) + \bar{f}(0)]/2$

Bennett et al⁽⁵⁾ have measured the regeneration amplitude in copper at an average momentum of 2.5 GeV/c; they found $|f - \bar{f}|/k = (2.17 \pm 0.06) \cdot 10^{-26} \text{ cm}^2$. This value has been used and the variation of $|f - \bar{f}|/k$ with momentum has been deduced from the article of Böhm et al⁽⁶⁾.

Values of $\sigma_D = 228\text{mb}$, $\sigma_T = 960\text{mb}$ and $\psi_{22} = 8^\circ$ have been used (see references 5 and 6).

All efficiencies for $2 \pi^0$ decays have been computed using a Monte Carlo program similar to the one described in reference (3). It should be emphasized that only the relative efficiencies are necessary for the analysis. The relative weightings at different momenta were deduced from the K_L^0 momentum spectrum, as measured by Böhm et al⁽⁷⁾ for the same production angle.

4.2 ANALYSIS WITH THE SIX REGENERATOR POSITIONS:

The measured events were selected according to the following criteria:

$$(a) \quad \chi^2_{\text{diff}} = \left[\left(\frac{E_\phi - E_{\gamma\gamma}}{0.2 E_{\gamma\gamma}} \right)_{\pi_1^0} - \left(\frac{E_\phi - E_{\gamma\gamma}}{0.2 E_{\gamma\gamma}} \right)_{\pi_2^0} \right]^2 < 2.0$$

(b) $1.65 \text{ GeV}/c < p' \text{ (measured momentum)} < 2.75 \text{ GeV}/c$

(c) Transverse momentum = $p' \sin \theta' < 0.1 \text{ GeV}/c$

(d) $\chi^2 = \left(\frac{E_\phi - E_{\gamma\gamma}}{0.2 E_{\gamma\gamma}} \right)^2 < 6.25$ for π_1^0 and π_2^0

(e) $|x'| < 6.5 \text{ cm}$, $|y'| < 5.75 \text{ cm}$; x' and y' are the horizontal and vertical distances of the decay point from the beam axis.

(f) $|x'_i| > 7 \text{ cm}$ for all four gammas; x'_i is the horizontal distance of the intersection of the gamma direction with the front plane of the spark chamber.

The first three criteria have been extensively discussed in reference (3). Criterion (d) eliminates the events which are not $2 \pi^0$ decays but give by accident a low value for χ^2_{diff} . Criterion (e) defines a fiducial decay volume; less than 10% of the events fell outside those limits. With criterion (f) the efficiency computations are independent of the counter A_4 veto efficiency.

Figure 2 shows the mass distribution obtained by applying those cuts on all measured events. The background has been drawn to fit the low and high masses; the statistics on the $3 \pi^0$ Monte Carlo are not yet sufficient to produce a mass distribution, and it has been assumed on the basis of Monte Carlo results for a previous experiment⁽³⁾ that the $3 \pi^0$ background varies smoothly around the K^0 mass. The mass distribution obtained after background subtraction fits well the Monte Carlo expectation for $2 \pi^0$ decays, including the slight asymmetry towards high masses.

Figure 3 shows the mass distributions obtained for each of the six regenerator positions; from position 6 to position 1 the regenerator moves upstream along the beam. The lead wall imposes a rather sharp cut-off to the decay region; therefore the percentage of the total background (Fig. 2) subtracted for each position was determined according to the monitor counts. These backgrounds fit with the number of events observed at low and high masses for each position.

The number of signal events in the mass interval 470 - 530 MeV/c² were deduced for each position. Integration of formula (1) over p, z, p' and z' for each z_R leads to the expected intensities (up to a normalization constant) as a function of ψ_{00} and $|\eta_{00}|$.

Figure 4 shows the best fit obtained, which gives:

$$\begin{aligned}\psi_{00} - \psi_f &= 56^\circ \pm 50^\circ \\ |\eta_{00}| &= (3.5 \pm 1.2) \times 10^{-3}\end{aligned}$$

The errors are statistical only. For fixed values of $|\eta_{00}|$ the error on ψ_{00} is 31°.

4.3 TIME DEPENDENCE OF $K_S - K_L$ INTERFERENCE IN THE $\pi^0 \pi^0$ CHANNEL

The events were selected with the same criteria as in 4.2, with the exception of (b) modified to include events from 1.5 GeV/c up to 3.5 GeV/c, to cover a time range as wide as possible.

An apparent time $\tau' = (z' - z_R) / 5.2 \rho'$ was defined for each event. Integration of formula (1) for fixed τ' leads to the expected τ' distribution as a function of ψ_{00} and $|\eta_{00}|$.

As in 4.2, the background was drawn on the observed mass distribution for all values of τ' . The ratio between the background in the mass interval 470 - 530 MeV/c² and the total background for the sum of the two intervals 410 - 470 MeV/c² and 530 - 590 MeV/c² was determined from that plot. For each τ' interval the background was then computed from the number of events in the two outside mass intervals using the ratio determined from the global mass plot. Consistent values of that ratio were obtained for mass plots corresponding to several momentum intervals.

Figure 5 shows the experimental data with the best fit obtained for the decay-time distribution of $K^0 \rightarrow 2\pi^0$ events. The chi-squared is 16.4 for 15 degrees of freedom. The fit gives:

$$\begin{aligned}\varphi_{00} - \varphi_f &= 67^\circ \pm 22^\circ \\ |\eta_{00}| &= (3.2 \pm 0.6) \times 10^{-3}.\end{aligned}$$

Figure 6 gives the chi-squared contours corresponding to 1, 2 and 3 standard deviations from the fitted values.

Monte Carlo calculations indicate a measurement accuracy of ± 9 cm for the decay point. The influence of the smearing was studied; a variation of ± 1 cm in the measurement accuracy changes the phase by $\pm 5^\circ$. The influence of a shift is more serious; if the origin of the z axis is moved by 1 cm, the phase varies by 13° . The geometrical reconstruction was checked by measuring fictitious rays converging to a known point. It was concluded that the error introduced by the geometry was less than ± 1 cm. However, a shift could be intro-

duced in the measuring procedure itself when fitting the directions of the showers on the scanning table. Extensive studies on the data for the initial life times ($-2 < \tau/\tau_s < 3$) lead to an estimate of ± 1.5 cm for the possible systematic error. The effect of those variations on the value of $|\eta_{00}|$ is always less than 5%.

Including systematic errors, the result of this analysis is:

$$\begin{aligned}\varphi_{00} - \varphi_f &= 67^\circ \pm 30^\circ \\ |\eta_{00}| &= (3.2 \pm 0.7) \cdot 10^{-3}\end{aligned}$$

5. CONCLUSION

The results of the two analyses are in good agreement. The second method, more sensitive to the interference term, gives more precise values.

Two measurements^(8, 9) of $\varphi_{+-} - \varphi_f$ have been made with a copper regenerator at a similar K^0 momentum. The average value $\varphi_{+-} - \varphi_f = 90^\circ \pm 10^\circ$ is combined with the results of the present experiment to give:

$$\varphi_{+-} - \varphi_{00} = 23^\circ \pm 32^\circ$$

The new value of $\varphi_f = -(44^\circ \pm 7^\circ)$, obtained from the experiment of Bennett et al⁽⁵⁾, and given by Steinberger at this conference, leads to:

$$\varphi_{00} = 23^\circ \pm 30^\circ$$

This result is evidence against T conservation with CPT violation; it favours strongly the solution of the Wu and Yang triangle with $Re \epsilon \approx 10^{-3}$ in the case of CPT conservation.

The result $|\eta_{00}| = (3.2 \pm 0.7) \cdot 10^{-3}$ is in agreement with the value of reference 3; it is also compatible with $|\eta_{+-}|$ within two standard deviations.

ACKNOWLEDGEMENTS

We thank Messrs. L. Bonnet, J. Olsfors and R. Schillsott for their efforts in building and running the apparatus. We are most grateful to M.A. Huber and the other scanners and measurers of CERN, Laboratoire de l'Accélérateur Lineaire and Rutherford Laboratory. We would like to thank Professors A. Blanc-Lapierre, G. Cocconi, A. Lagarrigue, P. Preiswerk and G.H. Stafford for support and encouragement.

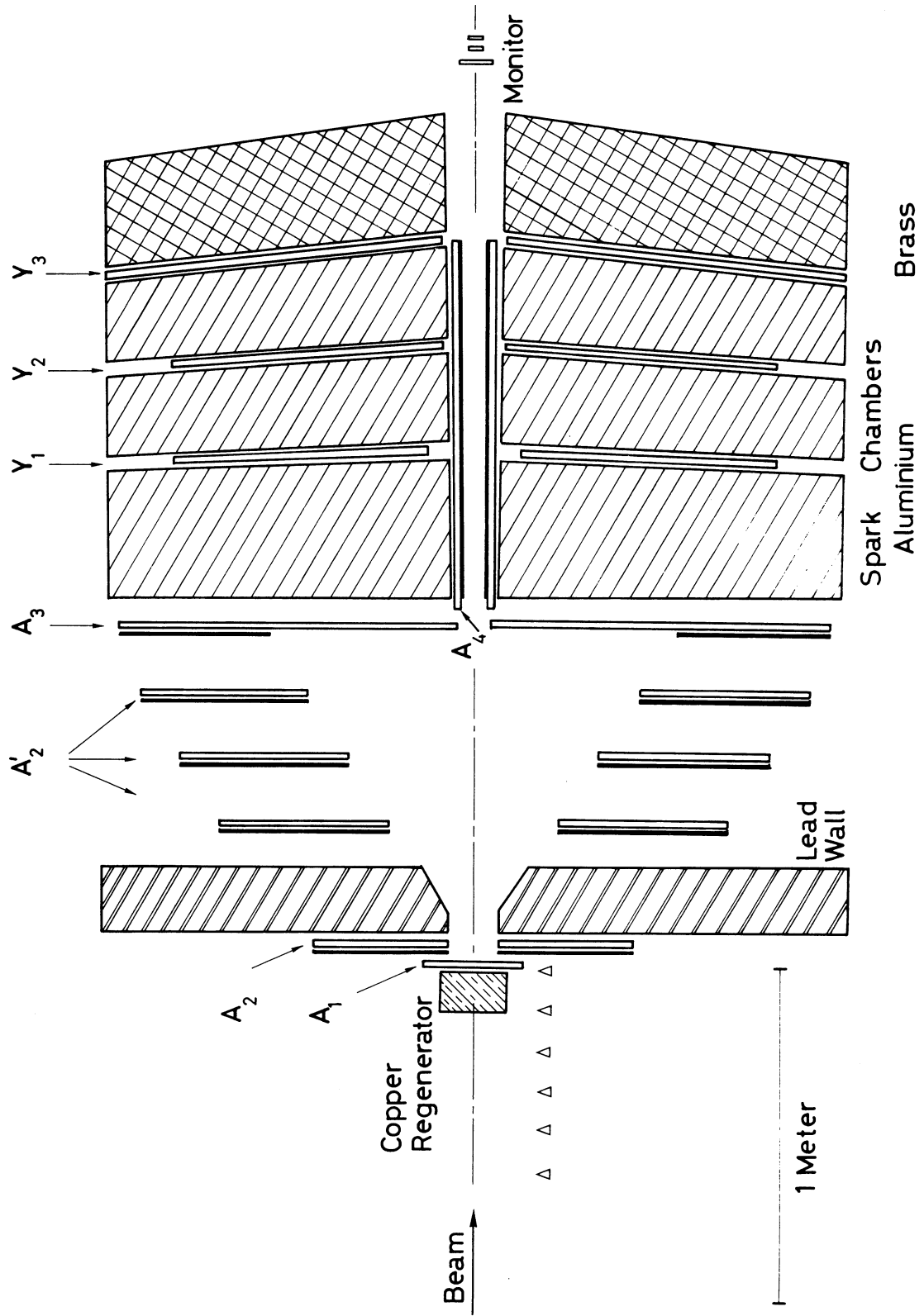


Figure 1 Experimental setup

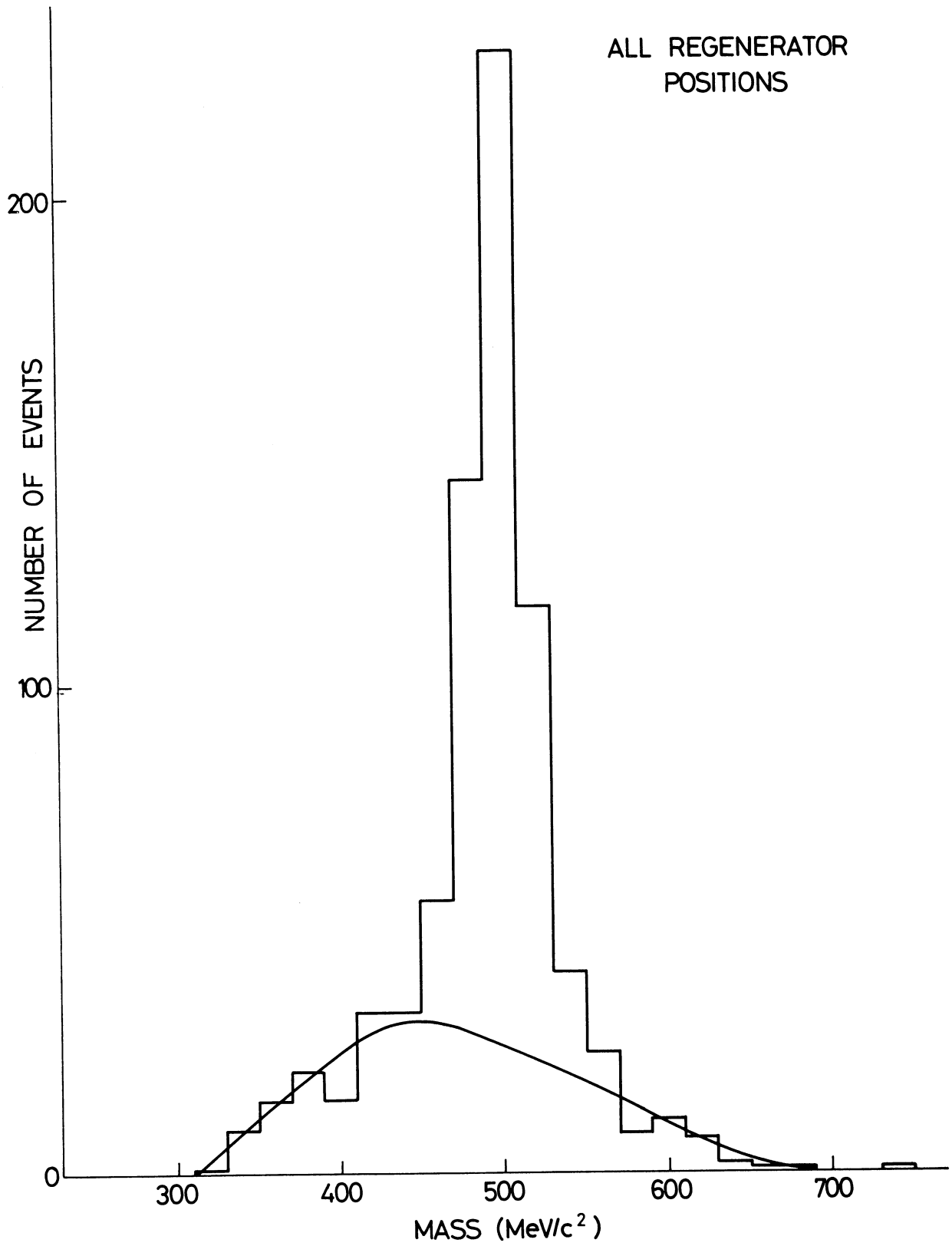


Figure 2 Mass distribution for all regenerator positions.

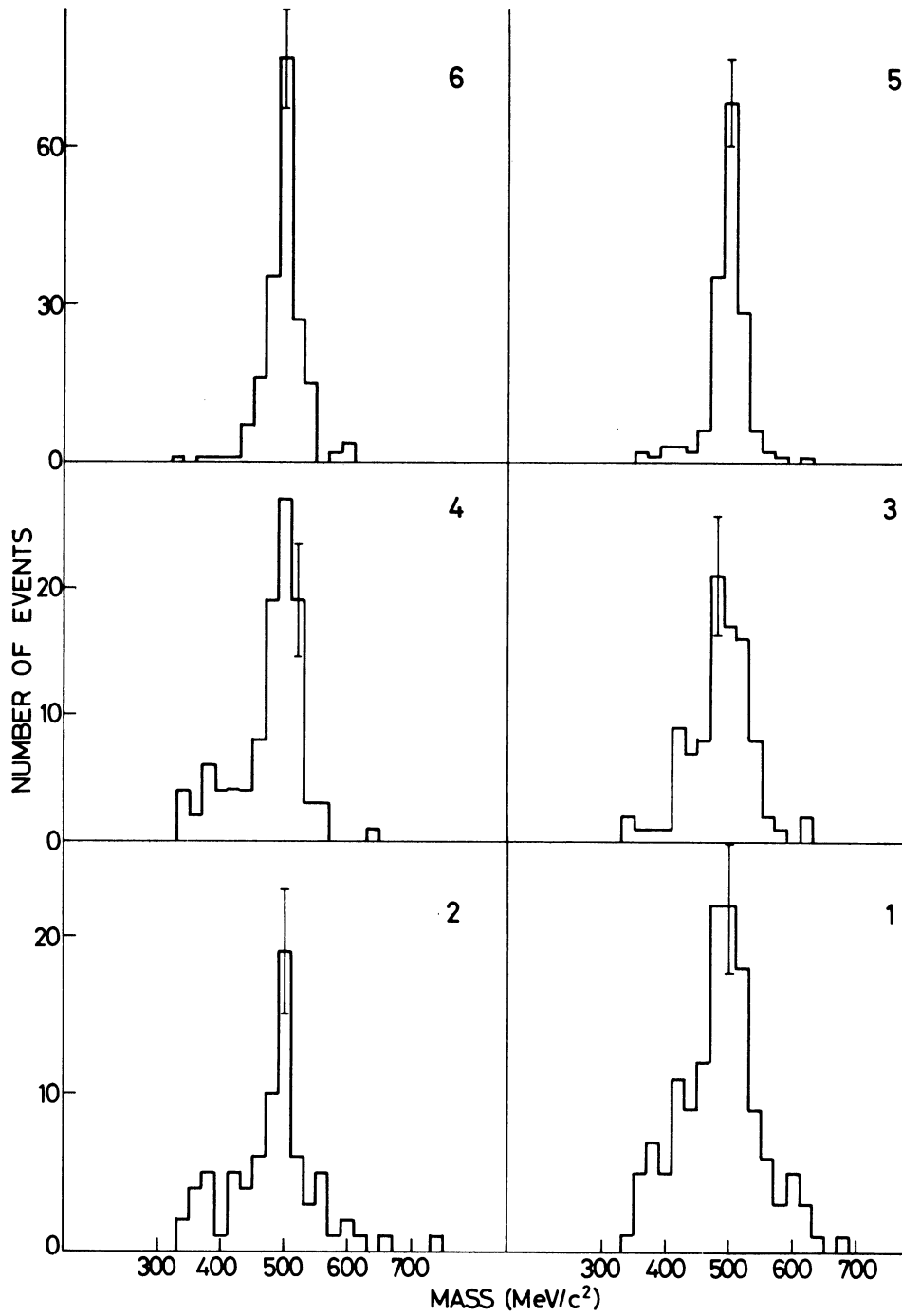


Figure 3 Mass distributions for each regenerator position.

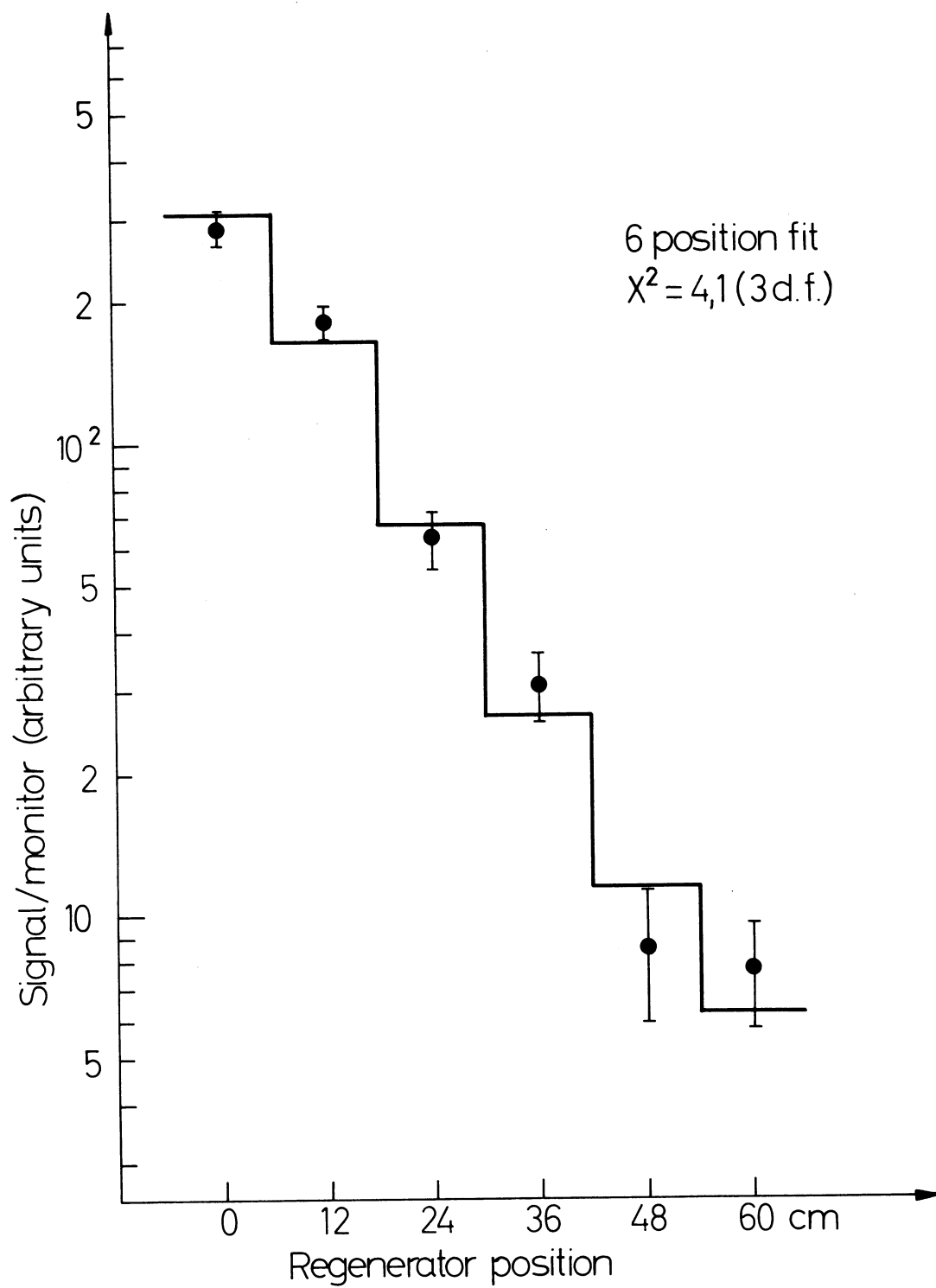


Figure 4 Experimental data and best fit for the six regenerator positions.

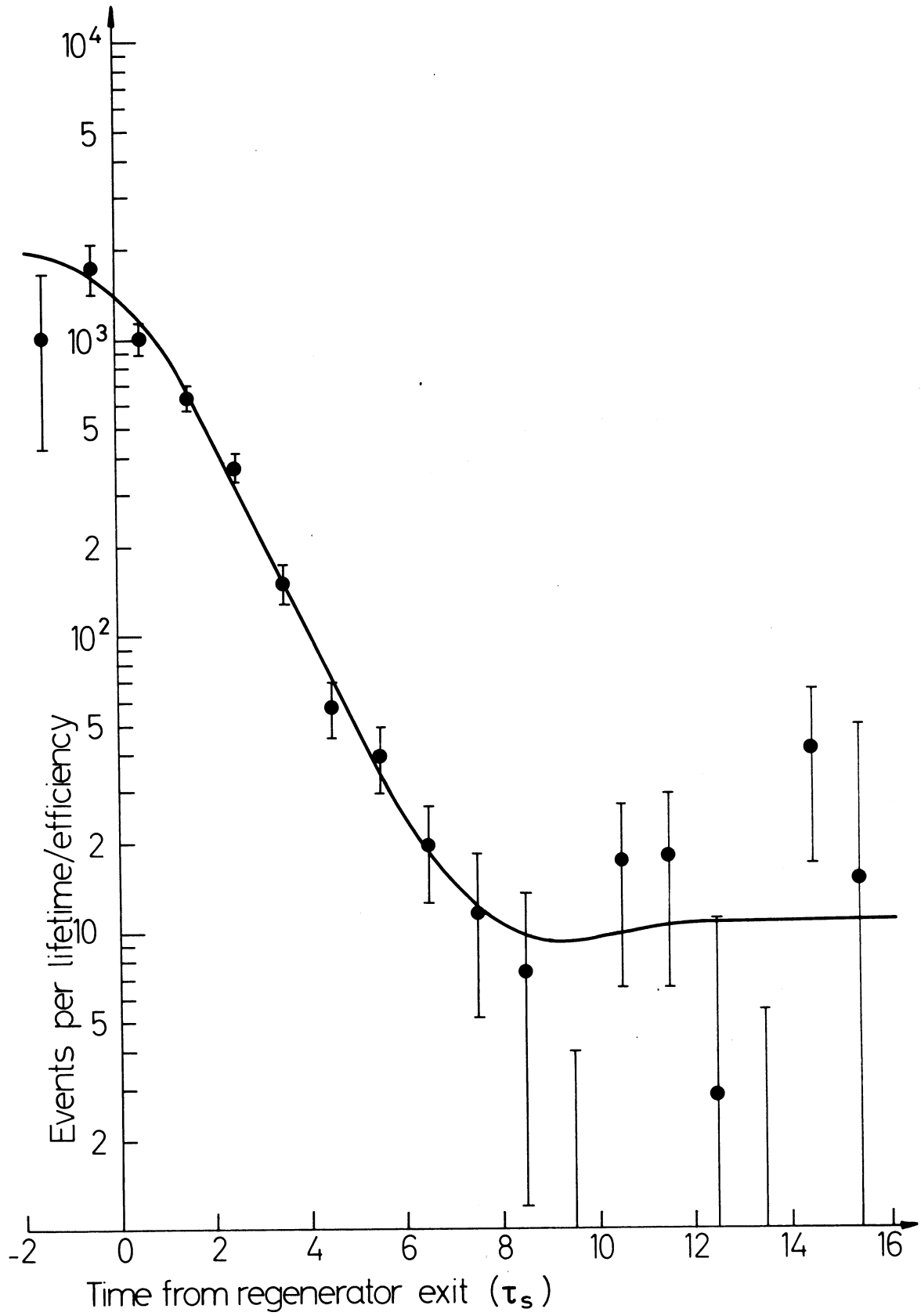


Figure 5 Experimental data and best fit for decay-time distribution of $K^0 \rightarrow 2\pi^0$ events.

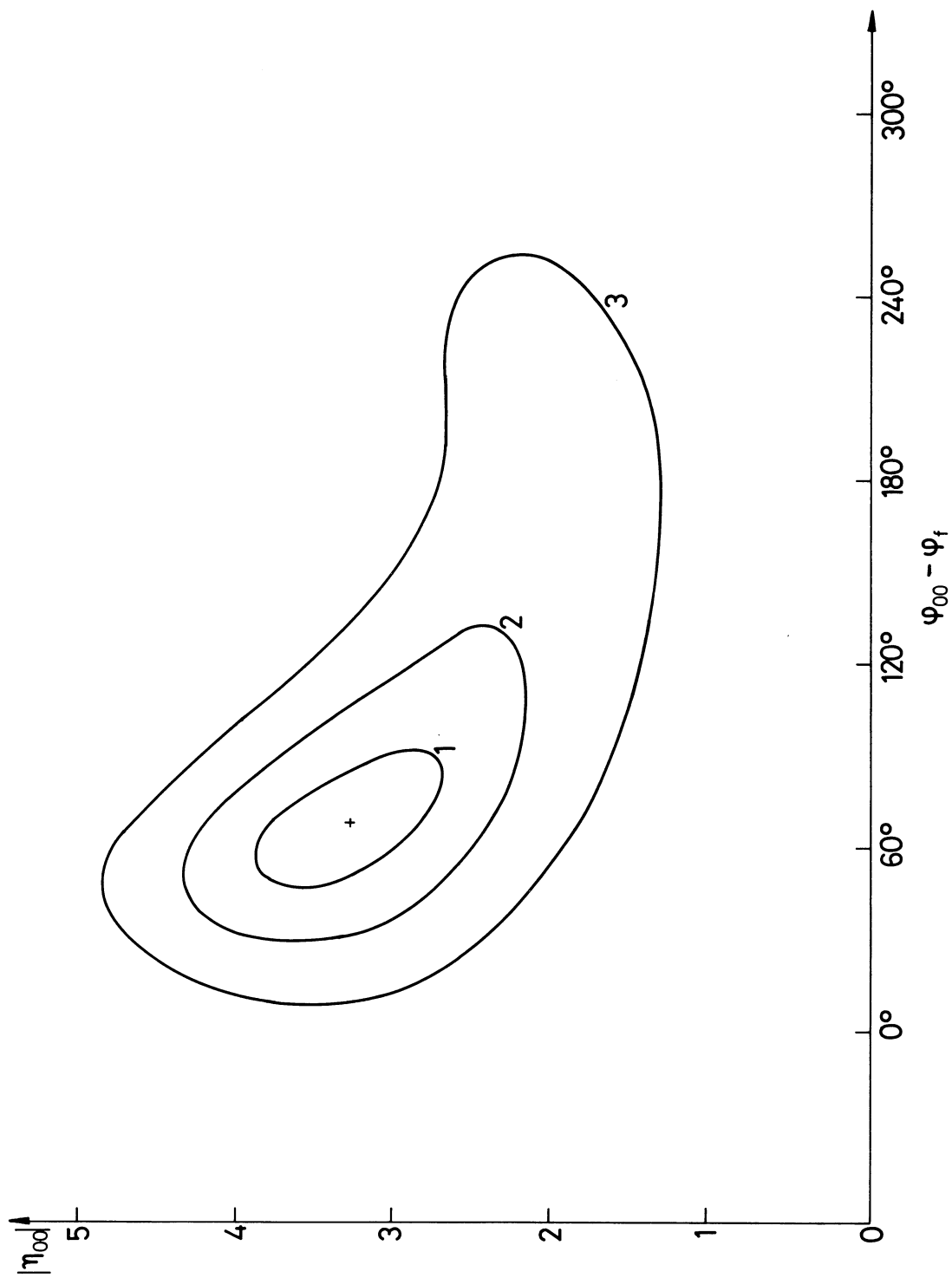


Figure 6 Chi-squared contours in the $\varphi_{00} - |\eta_{00}|$ - plane. The centre corresponds to the fit shown on Figure 5.

REFERENCES

- 1) T.T. Wu and C.N. Yang,
Phys.Rev.Letters, 13, 330 (1964).
- 2) H. Faissner, F. Ferrero, A. Ghani, E. Heer, F. Krienen,
G. Muratori, T.B. Novey, M. Reinharz and
R.A. Salmeron,
Nucl.Instr.Methods, 20, 213 (1963)
- 3) J-M. Gaillard, F. Krienen, W. Galbraith, A. Hussri,
M.R. Jane, N.H. Lipman, G. Manning, T.J. Ratcliffe,
P. Day, A.G. Parham, B.T. Payne, A.C. Sherwood,
H. Faissner and H. Reithler,
Phys.Rev.Letters, 18, 20 (1967).

J-M. Gaillard, W. Galbraith, A. Hussri, M.R. Jane,
N.H. Lipman, G. Manning, T.J. Ratcliffe, H. Faissner
and H. Reithler,
Nuovo Cimento, to be published.
- 4) R.H. Good, R.P. Matsen, F. Muller, O. Piccioni,
W.M. Powell, H.S. White, W.B. Fowler and R.W. Birge,
Phys.Rev., 124, 1223 (1961).
- 5) S. Bennett, D. Nygren, H. Saal, J. Sunderland and
J. Steinberger,
Phys.Letters, 27B, 239 (1968).
- 6) A. Böhm, P. Darriulat, C. Grosso, V. Kaftanov,
K. Kleinknecht, H.L. Lynch, C. Rubbia, H. Ticho
and K. Tittel,
Phys.Letters, 27B, 594 (1968).
- 7) A. Böhm, C. Grosso, V. Kaftanov, K. Kleinknecht, H.L. Lynch,
C. Rubbia, J. Steinberger and K. Tittel,
Private Communication.
- 8) C. Alff-Steinberger, W. Heuer, K. Kleinknecht, C. Rubbia,
A. Scribano, J. Steinberger, M.J. Tannenbaum and
K. Tittel,
Phys.Letters, 21, 595 (1966).
- 9) V. Bisi, A. Böhm, P. Darriulat, H. Faissner, M.I. Ferrero,
H. Foeth, C. Grosso, V. Kaftanov, K. Kleinknecht,
H.L. Lynch, C. Rubbia, A. Staude, J. Sandweiss,
K. Tittel,
Contribution 590 to the 14th International Conference
on High Energy Physics, Vienna 1968.